Dynamic Agent Based Simulation of an Urban Disaster Using Synthetic Big Data

A.Yair Grinberger[1] Michal Lichter[2] and Daniel Felsenstein[3]

[1] asherya.grinberger@mail.huji.ac.il Department of Geography, Hebrew University of Jerusalem Mount Scopus, 91900 ISRAEL

[2] mlichter@gmail.com Department of Geography, Hebrew University of Jerusalem Mount Scopus, 91900 ISRAEL

[3] msdfels@mscc.huji.ac.il Department of Geography, Hebrew University of Jerusalem Mount Scopus, 91900 ISRAEL

Abstract

This paper illustrates how synthetic big data can be generated from standard administrative small data. Small areal statistical units are decomposed into households and individuals using a GIS buildings data layer. Households and individuals are then profiled with socio-economic attributes and combined with an agent based simulation model in order to create dynamics. The resultant data is 'big' in terms of volume, variety and versatility. It allows for different layers of spatial information to be populated and embellished with synthetic attributes. The data decomposition process involves moving from a database describing only hundreds or thousands of spatial units to one containing records of millions of buildings and individuals over time. The method is illustrated in the context of a hypothetical earthquake in downtown Jerusalem. Agents interact with each other and their built environment. Buildings are characterized in terms of land-use, floor-space and value. Agents are characterized in terms of income and socio-demographic attributes and are allocated to buildings. Simple behavioral rules and a dynamic house pricing system inform residential location preferences and land use change, yielding a detailed account of urban spatial and temporal dynamics. These techniques allow for the bottom-up formulation of the behavior of an entire urban system. Outputs relate to land use change, change in capital stock and socio-economic vulnerability.

.

Keywords: Agent based simulation, earthquake, synthetic big data, socio-economic profiling

Acknowledgements; This research is partially based on work done in the DESURBS (Designing Safer Urban Spaces) research project funded by the European Commission FP7 Program under Grant Agreement # 261652.

1. Introduction

The routine management of cities requires information regarding population characteristics, infrastructure, land-use, house prices, commercial activity, and so on. In the advent of a hazardous event (both natural and man-made) these different, yet interrelated sub-systems demand an immediate response. Invariably, the data requirements for this are only available at a coarse spatial resolution, such as TAZs or statistical units. Different data may be available at varying scales and administrative divisions. Moreover, the spatial extent of the disaster will probably not neatly overlap these divisions. Therefore, urban disaster management requires data which is detailed and dynamic, spatially and temporally. While high resolution, big data for individuals is becoming increasingly available (such as geo-tagged social media data, mobile phones, GPS tracking etc) and free of arbitrary spatial configurations, these data often over represent eager-sharers and under represent the technologically-challenged. Furthermore these data often do not include crucial socio-economic profiling such as that provided by surveys.

In this paper we show how existing 'small' administrative data can be utilized to generate 'synthetic' urban big data. We emphasize that such synthetic data is essential for disaster management. Big data is generated by decomposing small areal units into households and individuals, profiling them with socio-economic attributes and combining this data with an agent based simulation model in order to create dynamics. We use a GIS buildings layer to disaggregate administrative small data into households, individuals and eventually to the level of the synthetic location of individuals within buildings by floors. The resultant data can be considered 'big' in terms of volume, variety and versatility. Potentially, it allows for different layers of spatial information to be populated and embellished with synthetic attributes. This process of decomposition facilitates moving from a database describing hundreds or thousands of spatial units to one containing records of millions of buildings and individuals over time. The result is a comprehensive set of spatial 'big data' in which every single individual in a city is synthetically represented by a set of socio-economic attributes and high frequency dynamics.

A popular approach to handling this synthetic data is to intersect it with hazard maps to create a visual dynamic account of the development of a disaster. We have done this elsewhere using a dynamic web-interface that combines flood-hazard maps with the socio economic attributes of the areas under threat (Lichter and Felsenstein 2012). Alternatively, this data can serve as input for dynamic agent based (AB) modeling of urban disasters. This paper illustrates the latter route. We use data fusion techniques at the level of the individual building to generate the initial starting population data for an agent based simulation of an urban disaster. These techniques allow for the bottom-up formulation of the behavior of an entire urban system.

The behavioral response of each agent is determined according to its socio-demographic profiling. For example age, income and car ownership may constrain, enable, or affect travel mobility, activity selection, and residential location choice. In this manner, the data animates the population analytics for a dynamic agent based simulation of an earthquake in Jerusalem. The AB simulation is based upon individual citizen agents and their interaction with the built environment and with each other. Feeding off the disaggregated data, individual buildings are characterized in terms of land-use, floor-space and value. Agents are characterized in terms of income and socio-demographic characters and are allocated to residential buildings. Using simple behavioral rules grounded in risk-evasiveness, satisficing behavior, and residential location preferences, along with a dynamic house pricing system that informs land-use dynamics, a detailed description of urban spatial and temporal dynamics is presented.

The paper proceeds as follows. After reviewing AB modeling applications for urban disasters, we outline the modeling framework and context of the study. We then describe how the big data is generated and coupled with the AB model. Simulation results are presented relating to change in land use, capital stock and socio-economic structure of the study area. To embellish the visualization potential of this data, we present some output in the form of dynamic web-based maps. Finally, we speculate on further developments derived from this approach.

2. Literature Review; AB Modeling for Disaster Management

Agent based modeling provides an appropriate framework for disaster management (Fiedrich and Burgdardt 2007). In an agent based world, autonomous entities (agents) behave according to a set of pre-programmed and simplistic, decision rules. The activities of multiple agents create a computable system in which the actions of individual agents affect each other and the system as a whole. The result is a complex network of behavior patterns that could not have been predicted by simply aggregating individual agent behavior. More importantly, such a system can be simulated and subjected to various exogenous shocks. It is no wonder therefore that a whole slew of disaster management situations have been subjected to AB simulations especially where human organization and learning patterns can be programmed into the response behavior of agents. These applications range from flooding (Dawson, Peppe and Wang 2011), wildfires (Chen and Zhan 2008), epidemics (Simoes 2012) to hurricanes (Chen, Meaker and Zhan 2006) and earthquakes (Crooks and Wise 2013). Much of this effort produces output that highlights the collective behavior of the agents. This can range from simulating the intervention of first responders, predicting human behavior under conditions of stress, anticipating traffic and infrastructure congestion due to human movement patterns and even simulating assistance efforts, post disaster.

Less attention has been paid to simulating the response of this behavior on the built environment. At the micro level of individual buildings and human response patterns, Torrens (2014) has shown how the use of highly granular models can yield rich detail of building collapse, agent-agent interaction and evacuation dynamics in the case of a simulated urban earthquake. This contrasts with the ‘dumb, coarse and cursory’ (Torrens 2014, p.965) nature of other AB models that try to reconcile human and physical processes. The spatial and temporal dynamics of such a situation that are animated by an AB model give rise to a huge volumes of information that while not intuitively recognized as 'big data' certainly qualify as such in terms of volume and variety.[1] At the broader, system-wide level of the urban area, Zou et al (2013) argue that the bottom-up dynamics of AB simulation become homogenized when looking at complex urban processes such as sprawl or densification. They propose a different simulation strategy to that commonly used in AB modeling. This involves 'short-burst experiments' within a meta-simulation framework. It makes for more efficient and accelerated AB simulation and allows for the easy transfer across different spatial and temporal scales. Elsewhere, we have also illustrated that complex macroscopic urban change such as land use rejuvenation and morphology change in the aftermath of an earthquake, can be suitably analyzed in an AB framework (Grinberger and Felsenstein 2014, 2015).

While the literature addressing urban outcomes of disasters and using agent-based modeling is limited, there is a larger ancillary literature that indirectly touches on this issue from a variety of traditions. Chen and Zhan (2008) use the commercial Paramics simulation system to evaluate different evacuation techniques under different road network and population density regimes. Another approach is to couple GIS capabilities to an existing analytic tool such as remote sensing and to identify disaster hot spots in this way (Rashed et al., 2007). Alternatively, GIS can be integrated with network analysis and 3D visualization tools to provide a realtime micro-scale simulation tools for emergency response at the the individual building or city block level (Kwan and Lee 2005). At a more rudimentary level, Chang (2003) has suggested the use of accessibility indicators as a tool for assessing the post disaster effects of earthquakes on transportation systems.

A particular challenge to all forms of simulation modeling comes from the inherent dynamics of AB simulation and the visualization of results that has to capture both spatial and temporal dimensions. In the context of big data, this challenge is amplified as real time processing needs to also deal with large quantities of constantly changing data. These are state of the art challenges that require the judicious use of computational techniques, relational databases and effective visualization. The literature in this area is particularly thin. In a non-AB environment, Keon et al (2014) provide a rare example of how such integration could be achieved. They illustrate an automated geocomputation system in which a tsunami inundation and the resultant human movement in its aftermath are simulated. They couple the simulation model with a web-based mapping capability thereby allowing the user specify input parameters of their choosing, run the simulation and visualize the results using dynamic mapping via a standard web browser. A mix of server-side and client-side programming is invoked that allows the user all the standard functionality of web-based mapping.

Our approach takes this integration one stage further. In addition to using AB simulation we do not just combine a simulation model with a web-based visualization capacity but also generate the synthetic big data that drives the model. Once derived, this data need to be spatially allocated. The literature provides various methods such

[1]While not calling this 'big data' as such, Torrens (2014) notes that the volume of locations/vectors to resolve for each object moved in the simulation is of the order of 10^{12} -10^{14}.

as population gridding (Linard et al 2011), areal interpolation which calls for 'creating' locations (Reibel and Bufalino 2005) and dasymeteric representation which uses ancillary datasets such as roads or night-time lights imagery to approximate population location (Eicher and Brewer 2001, Mennis 2003) An alternative approach, adopted here, is to distribute the data discretely without resorting to interpolation or dasymetric mapping by combining different sources of survey and administrative data to create population count data. The result is then spatially referenced creating local population count data by utilizing an appropriate spatial anchor. In spirit, this method is closest to Harper and Mayhew (2012a,b) where local administrative data are combined and geo-referenced by a local source of land and property data.

3. The Modeling Framework

As behoves big data, the modeling framework used here is data-driven. The process is outlined in Fig 1. Socio-economic data for coarse administrative units (small data) is disaggregated into buildings and individuals on the basis of a GIS building layer and then recombined into households. The resultant synthetic data gives an accurate socio-economic profiling of the population in the study area. Coupling this data with an AB simulation models adds both temporal and spatial dynamics to the data. The result is a multi-dimensional big data set that affords flexibility in transcending conventional administrative boundaries. Outputs relate to socio-economic change, change in land use and capital stock in the aftermath of an earthquake. To fully capture the richness of the data generated we use web-based mapping to generate extra visual outputs.

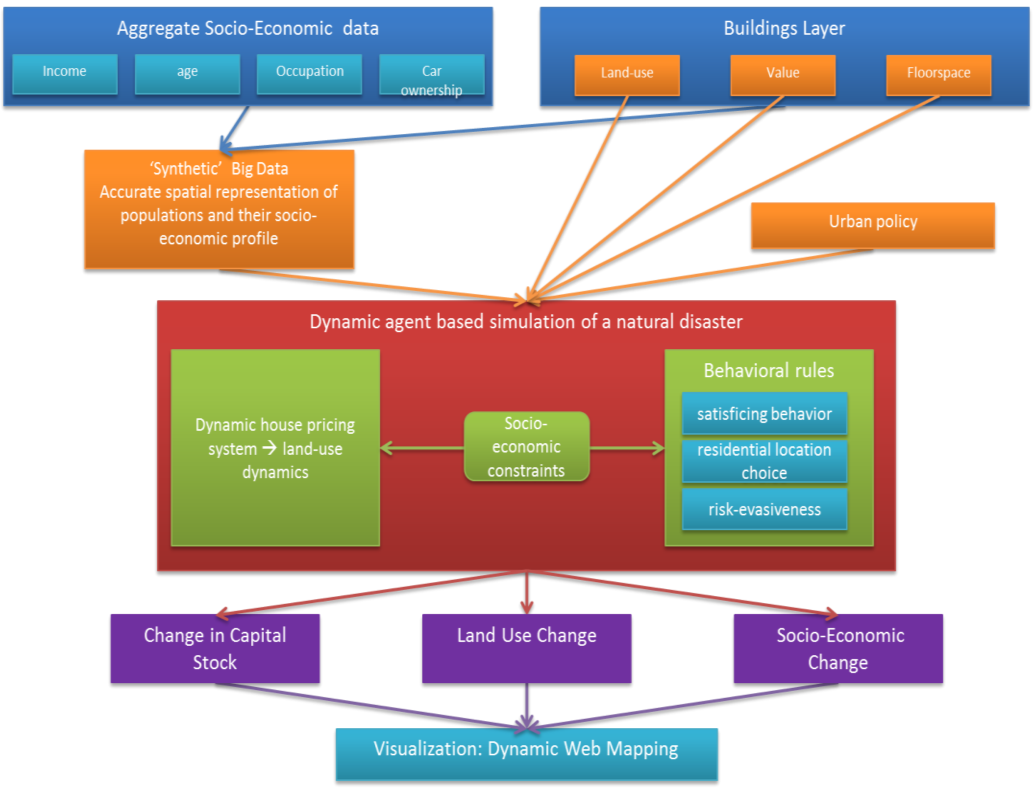

Figure 1: The modeling framework

The Context

We simulate an earthquake in downtown Jerusalem (Figure 2). While Jerusalem is located 30 km southeast of the active Dead Sea Fault line the last major earthquake in the city occurred in 1927. The city center lies in a relatively stable seismic area but many of its buildings were constructed prior to the institution of seismic-mitigation building codes making it prone to damage (Salamon, Katz & Crouvi, 2010). The study area houses 22,243 inhabitants, covers 1.45 sq km and is characterized by low-rise buildings punctuated by high rise structures. A heterogeneous mix of land uses exist represented by residential buildings (243Th sqm, 717 structures), commercial building s (505Th sqm, 119 structures) and government/public use buildings (420Th sqm, 179 structures). The area encompasses two major commercial spaces; the Machaneh Yehuda enclosed street market and the CBD. Three major transportation arteries roads traverse the area and generate heavy traffic volumes: Agripas and Jaffa Streets (light railway route) run north-west to the south-east and King George Street runs north-south. The area exhibits a heterogeneous mix of residential, commercial, governmental and public land use and high traffic volumes.

1 – CBD, 2 – Machaneh Yehuda Market, 3 – Jaffa St., 4 – Agripas St., 5 – King George St.

Figure 2: Study area

4. Big Data for Big Disasters

4.1 Generating Synthetic Big Data

Accurate spatial representation of data is essential for dealing with emergency situations in real time and for preemptive emergency management and training. However, spatial phenomena often do not neatly overlap administrative units of analysis. A need exists for accurately distributing the alpha-numeric socio-economic data for individuals or households within the spatial units used for data collection. We use a GIS-based system that allocates populations into buildings. We then create a spatial database where each inhabitant is represented as a unique entity. Each entity is attached a suite of unique socio-economic properties. Together, all the personal entities in every original spatial unit accurately represent the distribution of all socio-economic variables in the original unit. The disaggregation and reallocation process allows for the accurate spatial distribution of social and economic variables not generally available. This synthetically generated big data drives the AB simulation and underpins the unique characteristics of the agents. These characteristics will determine their behavioral choices.

The model is driven by data at three different resolutions: buildings, households and individuals. The original data is provided in spatial aggregates called Statistical Areas (SA)[2].This is the smallest spatial unit provided by the Israeli Central Bureau of Statistics (CBS) census[3]. We use a disaggregation procedure whereby spatial data collected at one set of areal units is allocated to a different set of units. This transfer can be effected in a variety of ways such as using spatial algorithms, GIS techniques, weighting systems etc (Reibel and Bufalino 2005). The GIS layer provides the distribution of all buildings nationally with their aerial footprint, height and land use. We derive the floor-space of each building and populate it with individuals to which we allocate the relevant socio-economic attributes of the SA to which they belong, according to the original distribution of these attributes in the SA. In this way, synthetic big data is created from spatial aggregates. The mechanics of the derivation are described in Appendix 1. The variables used to populate the buildings and drive the model are:

- Building level: land-use, floor-space, number of floors, building value, households
- Household level: inhabitants, earnings, car ownership
- Individuals level: Household membership, disability, participation in the work force, employment sector, age, workplace location.

[2] A statistical area (SA) is a uniform administrative spatial unit defined by the Israeli Central Bureau of Statistics (CBS) corresponding to a census tract. It has a relatively homogenous population of roughly 3,000 persons. Municipalities of over 10,000 population are subdivided into SA's.
[3] We also use coarser, regional data on non-residential plant and equipment stock to calculate non-residential building value. The estimating procedure for this data is presented elsewhere (Beenstock, Felsenstein and Ben Zeev 2011).

The variables used in the model, their sources and level of disaggregation appear in Table 1.

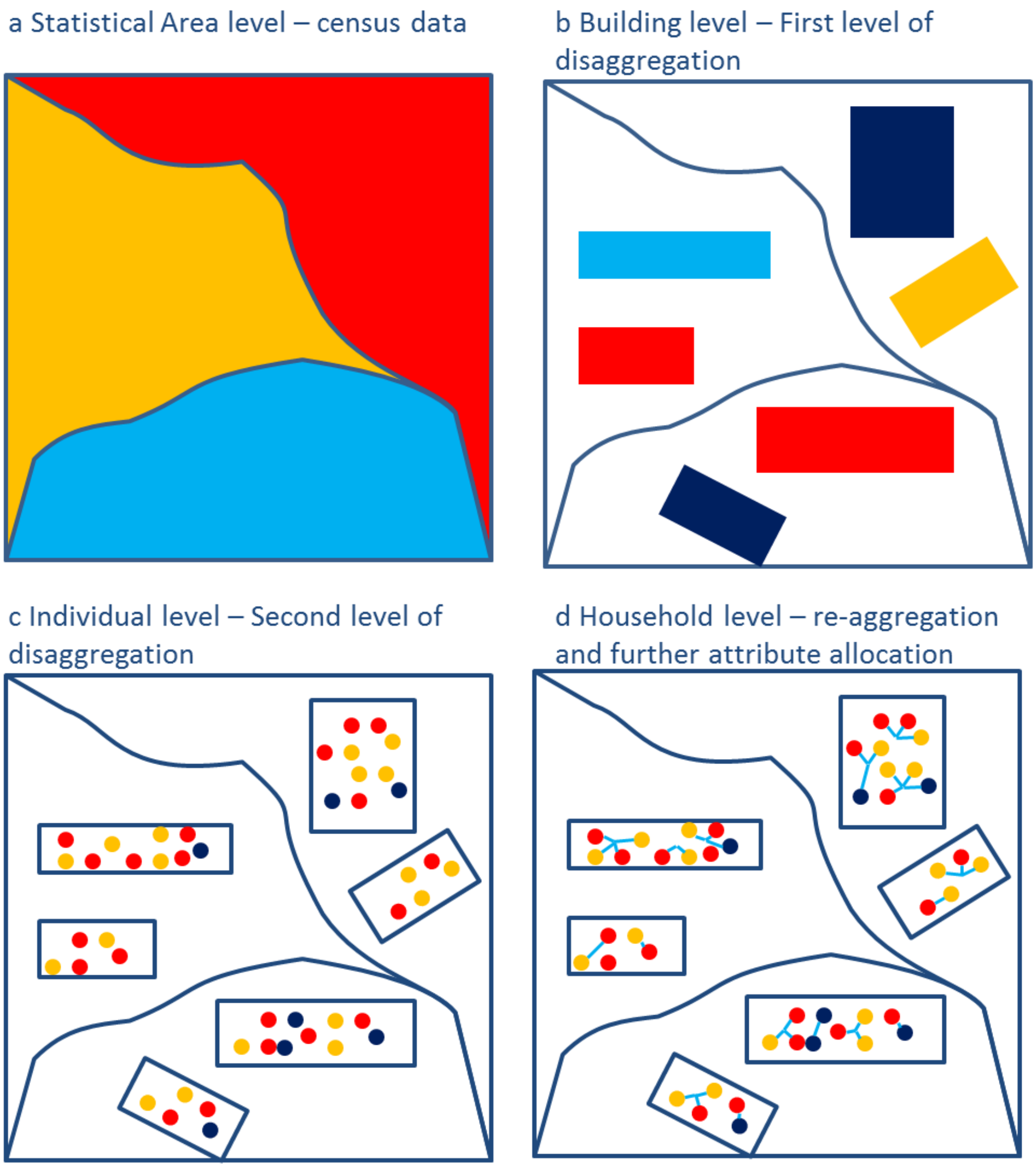

Figure 3: Data processing stages

Table 1: Variables used in the model

Variable	**Source**	**Spatial unit**	**Value**	**Disaggregation level**
Residential building Value per m^2	National Tax authority 2008-2013	SA	2008-2013 averaged (2009 real) value in NIS per m^2	Building
Non-residential plant value	Local authorities financial data (CBS)	Local authority	Total value of non-residential building stock in NIS per region	Building
Non-residential machinery and equipment value	Estimation	(Beenstock et al 2011)	Total value of non-residential equipment stock in NIS per region	Building
Number of households	CBS 2008	SA	Total number of households per SA	Building, household
Number of inhabitants	CBS 2008	SA	Total number of inhabitants per SA	Building, household, individuals
Average monthly household earnings	National Insurance Institute, annual data	Local authority	Average household monthly earnings by SA	Building, household
Labor force participation	CBS 2008	SA	Working / not working	Building, household, individuals
Employment by sector	CBS 2008	SA	Commercial / Governmental / Industrial / Home-based / Unknown	Building, household, individuals
% disabled	CBS	SA	% disabled in SA	Building, household, individuals
Age	CBS	SA	0-18 / 18-64 / 65+	Building, household, individuals
Workplace location	GPS survey 2014	survey of individuals	Inside the region / outside the region	individuals

Buildings Level disaggregation: The basis of the disaggregation procedure is calculating the floor-space of each building using height and land-use. We assume an average floor height of 5 m for residential building and 7 m for non-residential buildings (see Appendix 1). These figures are the product of comparing total national built floor-space (for each land-use) with total national floor-space as calculated from the building layer.

The entire data disaggregation procedure is automated using SQL and Python code and the results at each stage are stored in a spatial database. The process entails first allocating inhabitants into buildings and then assigning them socio-economic attributes. Later, these inhabitants are grouped into households and a further allocation of households attributes is performed. This necessarily involves loss of data due to dividing whole numbers (integers) such as households and inhabitants by fractions such as building floor-space for density calculations and percentages for socio-economic attribute distributions. In order to avoid loss of data and to meet the national control totals in each calculation, the SQL code is written so that it compensates for data losses (or increases) in the transition from floating points to integer values and ensures that the original control totals are always met. This is done by adjusting the floating point figures rounding threshold for each variable separately, to fit the losses or gain in the count of variables automatically.

Disaggregation at the level of the individual: The disaggregated building level data serves as the basis for the further disaggregation at the level of the individual. The building database includes a total of 1,075,904 buildings. A total of 7,354,200 inhabitants are allocated to 771,226 residential buildings. Disaggregation of the data to the individual begins with assigning each individual in the database a unique id, so that it is represented as a unique separate entity tied to a building in the database. Next, each person is allocated a random point location (a lat, lon coordinate) within the building with which it is associated. In each building, demographic attributes (labor force participation, employment sector, disabilities and age group) are allocated to each individual so that they comprise the entire distribution in the building which in turn gets its distribution from the SA in which it is located. In the same way, the distribution of work locations of inhabitants by employment sector is derived from a GPS-based transport survey carried by the Jerusalem Transport Master Plan Team (Oliveira et al., 2011). This is used to determine the distribution of inhabitants working inside or outside the study area according to their sector of employment and to assign the corresponding binary values to individuals

Household level clustering and attribute allocation: Individuals are clustered into households by size of the household in each building. This creates new unique entities in the database representing households. Households are associated with buildings, and inhabitants are assigned to them. The clustering introduces heterogeneity in terms of the age distribution in the household to closely represent a “traditional household” containing both adults and children when these are present. This is achieved by an algorithm iterating through inhabitants in each building sorted by age, and assigning them to households. Depending on the age distribution in the building, this algorithm clusters inhabitants in a building into closely age represented but not identical, households. Each household is assigned the SA average household earnings value. Other attributes such as car ownership are assigned to households in the same way.

4.2 Coupling the Data with the Agent Based Model

The high resolution data detailed above is combined with an agent-based model. As agents represent the focal catalysts of change and aggregate patterns are decomposed into actions of individual agents, this further unshackles the constraints imposed by data collected on the basis of arbitrary administrative borders. In the context of the current study this allows us to relate to the specific spatio-temporal nature of the event and its long-term impacts. To do this we characterize the three basic elements of an AB model: agents, their environment and rules governing agent-to-agent and agent-to-environment interactions (Macal & North, 2005).

The data provides the first two with individuals and households as agents and buildings as the urban environment. The model itself reflects the dynamics of the urban system via a collection of simplistic behavioral rules. These govern the interactions within the system at each iteration (Fig 4) which is set to represent one day and also include an exogenous shock in the form of the earthquake. These rules are described in Appendix 2.

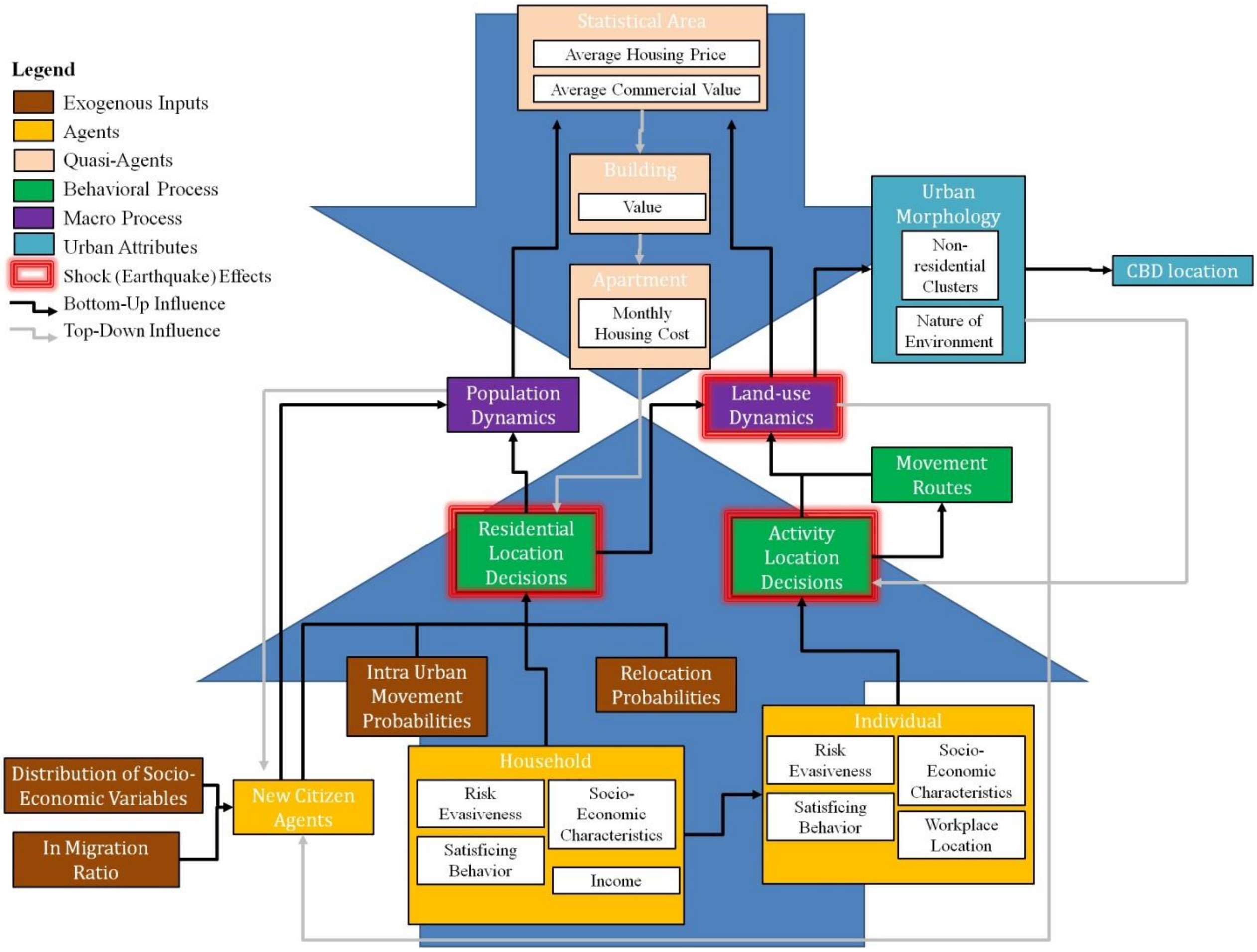

Figure 4: Conceptual formulation of agent-based model of an earthquake in a city

A simulation entity is created to represent each individual, household and building along with its spatial and socio-economic characteristics. Identifying the unique workplace for each employed individual in the study area is done on the basis of satisficing behavior. The first building which satisfies randomly generated preferences in terms of distance from home location and floor-space size (assuming larger functions attract more employees) and is of the land-use associated with the individual's employment sector is designated as the agent's workplace.

Agent behavior (bottom-up procedures): This simulation characterizes the city as a spatial entity whose organization emerges from the aggregate behavior of all its citizens (individuals). Individuals and households are therefore identified as the agents of the urban system. Their behavior is simplified into two decision sets: the decisions of households about place of residence and the decisions of individuals about choice and sequence of daily activities.

The decision to change place of residence is probabilistic and based on comparing a randomly drawn value to exogenous probabilities of migrating out of the study area (city-level probability), or relocating to another part of the study area (SA specific probability)[4]. Choosing a new place of residence location follows two decision rules: a willingness to commit up to one third of monthly household earnings to housing and preferences regarding the socio-economic characteristics of the residential environment. This follows a probabilistic and satisficing procedure similar to that described for selection of work place. If a household fails to find an alternative place of residence after considering 100 possible locations, it leaves the study area. Individual agents that are members of the household relocate/migrate with the household. In-migration is treated in the model by having the number of potential migrating households dependent on the number of available housing units and an exogenous in-migration/out-migration ratio. New households with up to 2 members are comprised of adults only. Those with more members include at least one non-adult agent and their socioeconomic status reflects the urban average for key socio-economic attributes.

At each iteration individuals conduct a variety of activities within the study area. These are important for land-use dynamics and the mobility paths between land uses (see below). The number of activities undertaken ranges from 0-11 and varies by socio-economic characteristics (age, car ownership of household, disability, employment status, location of employment) and randomly generated preferences. The location of each activity (with the exception of work activity for agents employed within the study area) is determined by the attractiveness of different locations. This in turn is dependent on floor-space size, environment, distance from previous activity, and the mobility capability of the individual. This choice criteria is again, probabilistic and satisficing. Movement between each pair of activities is not necessarily shortest-path. A more simplistic aerial-distance-based algorithm is used to reduce computing demands and again reflect the satisficing nature of agents[5].

Environmental influences (top-down procedures): AB models typically have a demand side emphasis characterizing the urban system as the outcome of residents' behavior. In normally functioning markets this means that agents will look for cheaper housing. On the supply side however, contractors will tend to build where prices (profits) are high and thus house prices will vary directly with population and

[4] Calculated from 2012 immigration data in the Statistical Yearbook for Jerusalem 2014 (Jerusalem Institute for Israel Studies).

[5] The algorithm works as follows: at each step, junctions adjacent to the current junction are scanned and the junction with the shortest aerial distance to the destination is flagged as the current junction for the next step. If a loop is encountered, it is deleted from the path. The algorithm ends when agents arrive at the junction closest to the destination or when all junctions accessible from the origin are scanned.

inversely with housing stock. In AB models the supply side is often overlooked. We formulate a top-down process in order to get a fuller picture of the operation of urban markets. We conceptualize administrative units, buildings and individual housing units as quasi-agents. These entities are not autonomous or mobile but are nevertheless sensitive to changes in their environment according to pre-defined rules of influence (Torrens 2014). Foremost amongst these are sensitivity to the distribution of commercial activity and to values of buildings. In this process, changes on the demand side (population dynamics), and related changes to the land-use system create effects which trickle down from the level of the administrative unit to the individual dwelling unit and ultimately to the individual resident.

We assume that the larger a commercial function, the more activity it will require in order to be profitable. We further assume that the volume of activity is represented by the intensity of traffic in the vicinity of each function. Consequently, traffic volume on roads near commercial functions should be proportional to their floor-space. Hence, any function that is not located near sufficient traffic will not survive and residential uses near large traffic volumes may change their function to commercial, forcing residents to relocate or migrate.

Changes to a dwelling unit's value represent a top-down spatial mechanism based on supply and demand dynamics. Average price per meter is pre-specified at the beginning of the simulation for each SA, for both residential and non-residential uses. As land-use and population dynamics change, supply and demand shift causing these average prices to fluctuate. We assume that non-residential value is affected only by changes in the supply (short supply drives prices up) while residential values are also sensitive to changes in demand (prices drop when population decreases). Changing average prices cause a change in building values according to floor-space. In the case of residential buildings this change is also effected through accessibility to services. Accessibility relates to the share of non-residential uses from total uses accessible from the building. A building whose accessibility is higher than the SA average will be higher priced. These effects further trickle down to the monthly cost of housing per dwelling unit. We assume uniformity of unit prices within a building meaning that the cost of each unit is the average cost of units in the building. This cost affects household residential choice in the next iteration.

The earthquake: this is formalized as a one-time shock, spreading outwards from a focal point with intensity decaying over distance. This earthquake is programmed to occur on the 51th simulation iteration, so the system has a sufficient 'run-in' period in which all processes initiate themselves and stabilize. The epicenter of the quake is determined randomly so that aggregate average results do not represent any place-based bias. As the impact spreads across space it may inflict damage to the environment. The probability a building being demolished as a result of the shock is proportional to both distance from the epicenter and height. A demolished building causes the nearest road to become unavailable for travel until the building is restored to use. The restoration period is proportional to the building's floor-space volume.

5. Simulation and Results

Results are presented relating to three main themes: land use change, change in value of capital stock and socio-economic change. These reflect three dimensions of urban vulnerability to unanticipated shocks: functional, economic and social vulnerability respectively. The simulation is run 25 times each with a duration of 1000 iterations (i.e. days). The earthquake occurs on day 51 in each simulation and is located randomly within the study area. The 50 day run-in time is heuristically derived, comprising of a 30 day period for stochastic oscillation and a further 20 day period for 'settling down'. Like any catastrophic change, the initial impact of the earthquake is an immediate population loss and damage to buildings and infrastructure. Yet as the results illustrate, these lead to a second, indirect round of impacts induced by the way in which agents react to the new conditions created.

Traffic Patterns and Land Use Change: we present a series of maps that illustrate change in land use (from residential to commercial and vice versa) and the concomitant dispersal of traffic activity at discrete time points (Figures 5 & 6). As can be seen, in the period following the disaster the main commercial thoroughfares running N-S and E-W across the area lose their prominence induced by changing movement patterns. Within 50 days of the event, major traffic loads shift from the north-west part of the study area into the south and to a lesser extent to the north-east and central sections. Commercial activity responds to this change and a cluster of medium-sized commercial uses appears in the south-west. However, by day 500 we observe a reversal of this pattern. Evidently, the recovery of the traffic network, along with the anchoring effect of large commercial land uses, helps Agripas St. to regain its position causing a new commercial cluster to develop in its vicinity. The immediate, post disaster change in traffic pattern does however leave a permanent footprint. Commercial land use becomes more prevalent in the north-east and CBD centrality seems to be slightly reduced. The buildings containing these activities have larger floor-space area than those located in the new emerging commercial clusters. This implies a potentially large addition of dwelling units to the residential stock in the case that these buildings transform into residences. One year after the shock these patterns hardly change as the new transportation pattern gets locked in, empty buildings become occupied and the potential for land use change is reduced. From the 3D representation of frequency of land use change (Fig 6) we can identify the time juncture where buildings that were previously empty become occupied. Between day 500 and day 1000 land use tends to become rejuvenated in the sense that unoccupied buildings become populated.

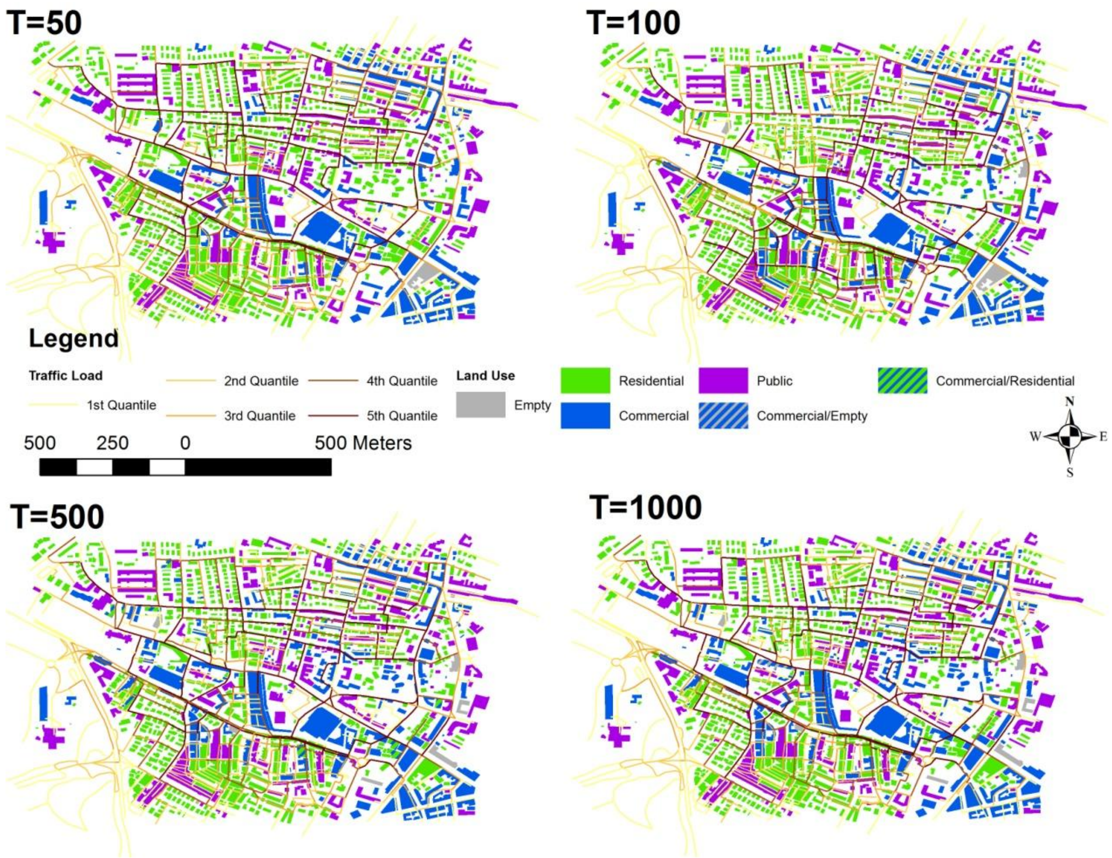

Figure 5: Average land-use maps at discrete time points

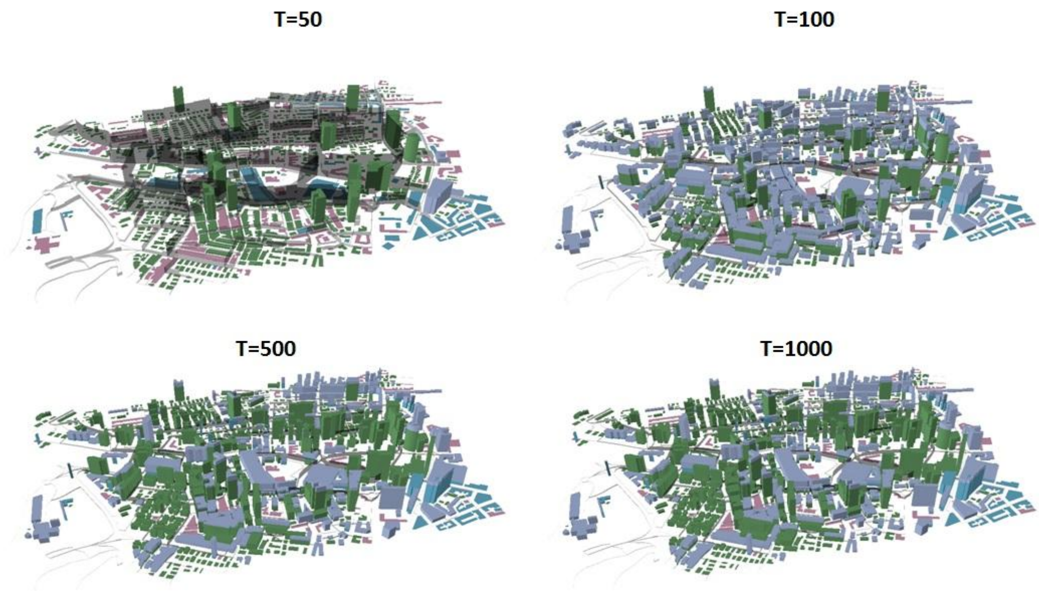

Figure 6: Frequency of land-use change at discrete time points

Frequency is represented by building height. Building color represents initial use. Colored section represents the share of total simulations in which the building was in use other than the original use, at that time point. Grey represents the share of times the building was unoccupied. Road height represents absolute traffic volume, while shading represents relative volume within the distribution of all roads.

Change in the Value of Capital Stock: standard urban economic theory suggests that demand for capital stock (residential and non residential) is inversely related to price while the supply of capital stock is positively related to price. In our AB world with dynamic pricing for both residential and non-residential stock, demand changes through population change and supply changes through either building destruction or change in land use as a result of changing traffic loads and accessibility to services. Aggregate simulation results for residential capital stock show that the number of buildings drops to about 600 after about 100 days and in the long run never recovers (Figure 7). However average residential values tend to rise only after 500 days to about 90 percent of their pre-shock values. This lagged recovery may be attributed to supply shortage and increased access to services as suggested by the changing land use patterns noted above along with increasing demand from a growing population. Yet, the fact that a reduced residential stock recovers to almost the same value suggests that this is due to rising average floor-space volumes. This would point to buildings that were initially large commercial spaces becoming residential. Non residential stock behaves rather differently. Long-term increase in stock is accompanied by lower average values. In contrast to residential stock, the turning point in these trends is after roughly one year (Figure 8). Elsewhere we have identified this with the dispersal of commercial activities from large centers to smaller neighborhood units (Grinberger and Felsenstein 2014). The current results reflect a similar picture. The number of units grows but their average value decreases as the buildings in the south-west and north-east have smaller floor space.

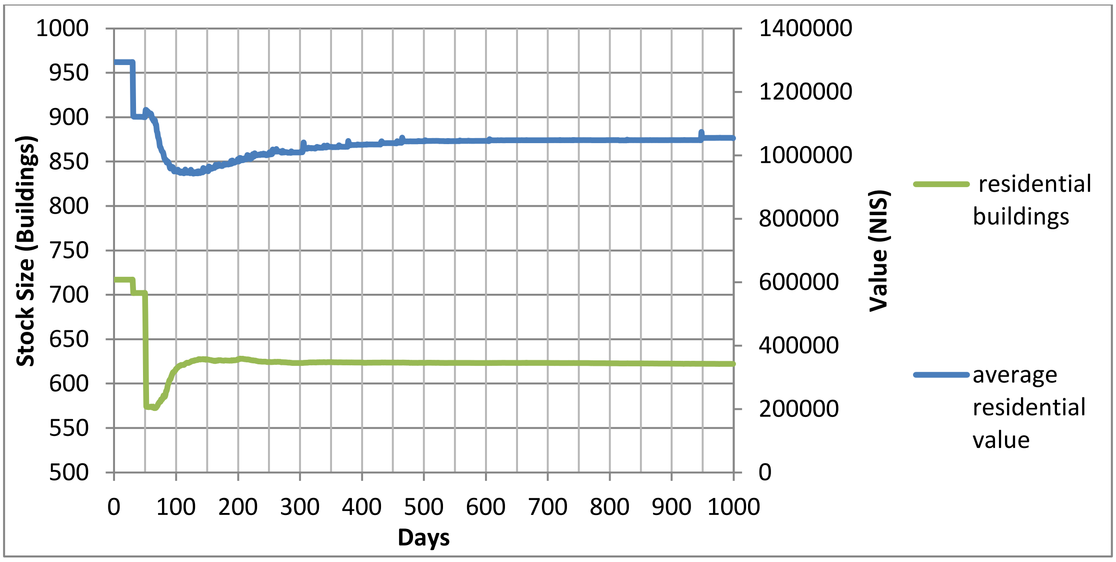

Figure 7: Change in residential capital stock

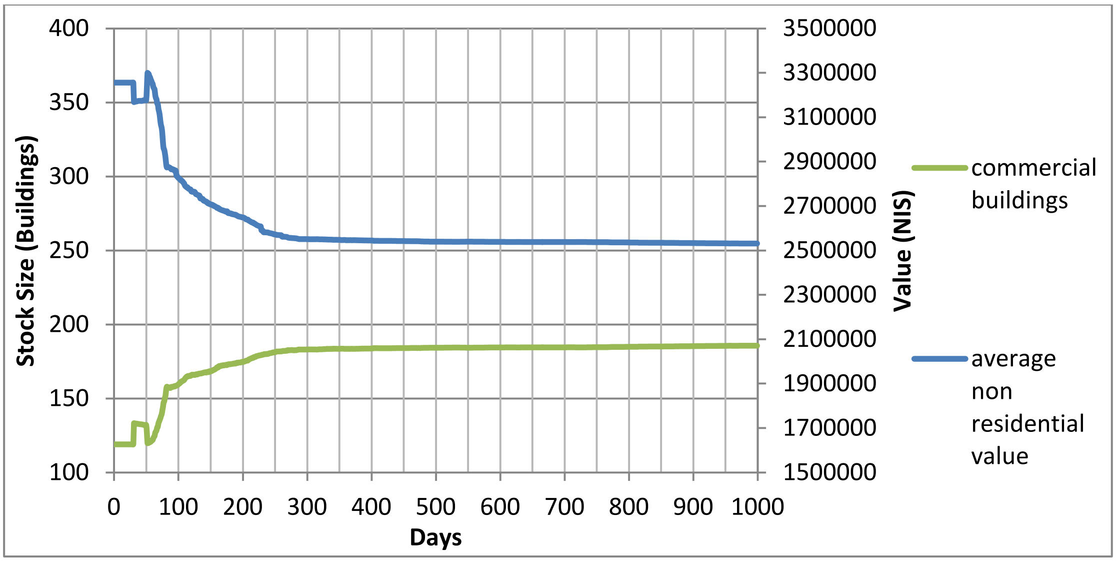

Figure 8: Change in non-residential capital stock

Population Dynamics: The initial impact causes a population loss of about 4,000 residents (Figure 9). After about one year population size recovers and continues to grow to about 29,000 by the end of the simulation period. This increase is the result of in-migration of an heterogeneous population with stochastic earnings. The ability of this extra population to find residence in the area is due to the process of land use change described above. The new, large residential buildings (previously commercial spaces) contain many individual dwelling units. While the average price of buildings rises, the rising average floor-space of buildings pushes down the average cost per dwelling unit within the building and consequently the monthly cost of housing services. As a result, lower income households find suitable lower cost residential location making for an increased population that is poorer on average. Since the average income of new in-migrants is slightly higher than the average income of the area, this suggests that the lower average income must result from the out-migration of wealthier households that accompanies in-migration.

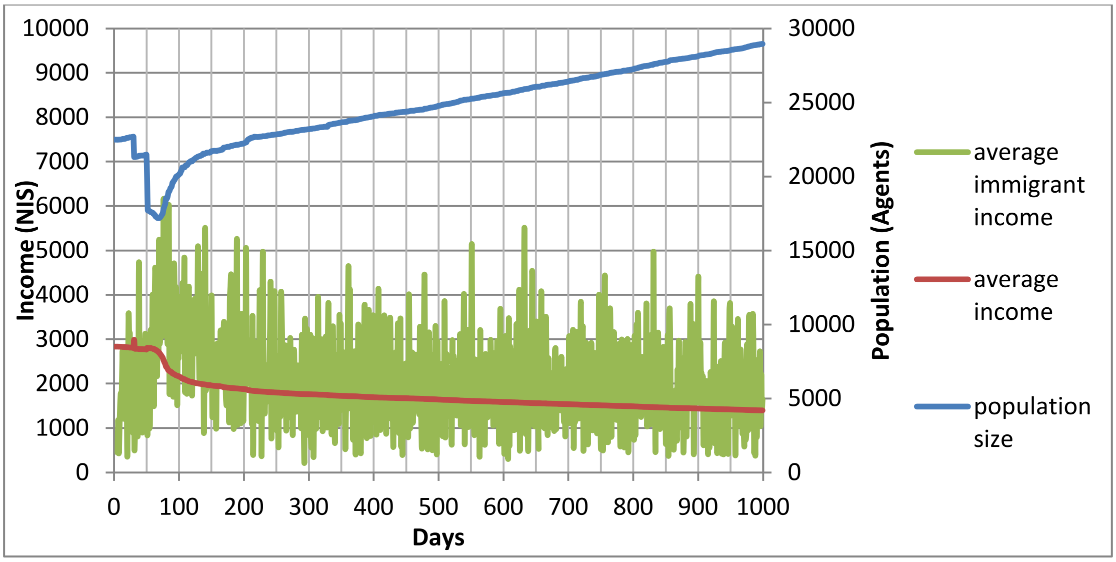

Figure 9: Population and income change

A composite indicator of both social, functional and economic vulnerability can be obtained by looking at the flow-through of households through buildings. The simple ratio of in-coming to out-going households per building at each discrete time step, gives an indication of the amount of through-traffic per building and an indication of its population stability. Fig 10 gives a summary account of this ratio. A high 'pull' factor is not necessarily a sign of stability or even attractiveness. It may be an indicator of transience and instability. The overall picture is one of unstable population dynamics. The simulations suggest that none of the buildings that were initially residential are consistently attractive to population. Most of them have difficulty maintaining their population size, post earthquake. For many buildings this is due to either physical damage or change in function for example, from residential to commercial use. It seems that only new potential residential spaces that start initially as commercial uses, consistently succeed in attracting population. The direct and indirect effects of the shock generate much household turnover (or 'churning') through buildings but without any indications of location preferences for specific buildings or parts of the study area. Total floor space that registers net positive household movement (strong/weak pull) amounts to only 75%of the floor space that registers net negative turnover (strong/weak push). This underscores the high state of flux in the study area.

Figure 10: Household movement through buildings

Social Vulnerability: a more in-depth examination of population movement is presented in Figure 11 where snapshots of the spatial distribution of social vulnerability at different time steps are presented. We follow Lichter and Felsenstein (2012) and use a composite index of social vulnerability[6]. Green indicates less vulnerable population and red more vulnerable. The average index value for each building is calculated, disaggregated into households and used to generate continuous value surfaces using Inverse Distance Weighting (IDW). The parameters used for the interpolation are: pixels of 10X10 meters, 100 meters search radius and a 2nd order power function.

Akin to movement patterns, residence patterns in day 100 present a process of dispersal as relatively less vulnerable households initially clustered in the west move eastward. This population is higher income and consequently has greater availability of resources for relocation. Since agents are characterized by limited tolerance to change it is not surprising to find that the destinations chosen by households are those that were better-off in the pre-event situation (light green areas). Residential patterns re-cluster after day 100, a process similar to the stabilization of traffic and land-use patterns. However, this re-clustering germinates a new spatial pattern with small

[6] Social vulnerability by household (V_{hh}) is defined as:
$V_{hh} = 0.5 * Z_{i_{hh}} - 0.2 * Z_{age_{hh}} - 0.2 * Z_{\%dis_{hh}} + 0.1 * Z_{car}$ where: Z is the normalized value of a variable, i is household income for household *hh*, *age* is the average age group of members of household *hh*, *%dis* is the percent of disabled members of all members in household *hh*, *car* is car ownership for household *hh*.

cluster of stronger population serving as nuclei for future agglomeration. These clusters attract households of similar characteristics resulting in the emergence of new clusters and a general process of entrenchment. This process occurs at a high spatial resolution that is much more granular than the SA level. Visualizing at this scale prevents the homogenization of patterns. For example, we can detect dispersion over time of the high vulnerability population as the east-west vulnerability patterns in the pre shock era becomes replaced by a much more heterogeneous picture.

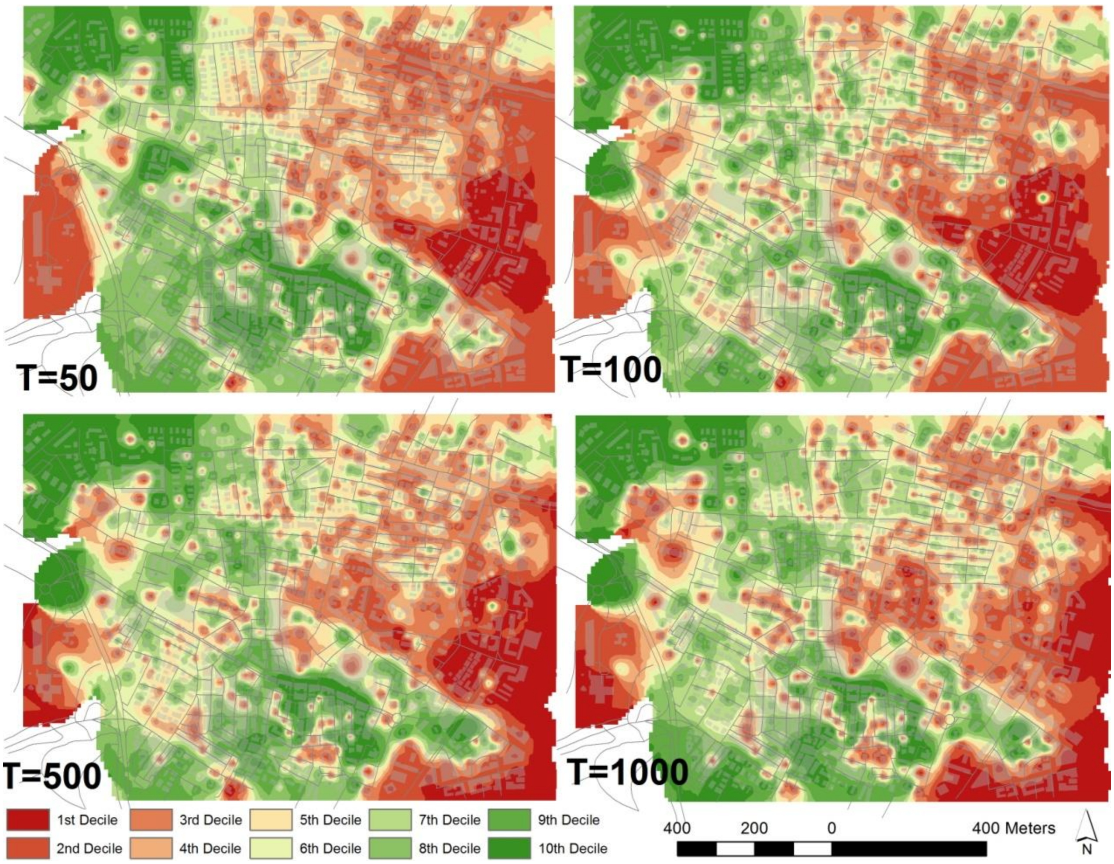

Figure 11: Social vulnerability heat map

6. Web-Based Delivery of Outputs

The richness of outputs is hard to envision and to communicate. The volume and variety of the big data used as input into the model is manifested in the complexity of these outputs. Not only are these produced for variables at different spatial units but they are also generated temporally for each variable. These dynamics are typically non- linear. The nature of the information generated necessitates a visualization technique capable of accommodating large amounts of data and presenting them spatially and temporally. This in turn means sophisticated database construction that will allow not only the dynamic representation of data but also the querying of data in a user-friendly fashion. We view this as a crucial linkage between the simulation outputs generated in a research oriented environment and their use by potential consumers such as planners, decision makers and the informed public.

The results are thus presented via a web-based application. This allows for communicating outcomes in a non-threatening and intuitive way (see http://ccg.huji.ac.il/AgentBasedUrbanDisaster/index.html). Using a web browser, users can generate results for different points in time and for different areas without prior knowledge of handling spatial data or GIS. They can choose a variable of interest, visualize its change over time and space and generate the relevant location specific information they need. To this end, we create a dedicated database for the output results of time series from the model simulation. This needs to be carefully constructed and sometimes does not follow strict DB design but rather contains some flat tables of lateral data in order to be displayed in pop-ups graphs and charts. The visualization includes time lapse representation of human mobility (household level), changes in passengers along roads, changes in buildings' land use and value, household socio-economic attributes change etc. in the study area (Figures 12-13).

We use Google Maps API as the mapping platform and add middleware functionalities. These are functions that are not provided by the mapping API but interact with it to provide ancillary capabilities (Batty et al. 2010) such as time laps animation, sliders, interactive graphs etc. These middleware functionalities are User Interface (UI) features that allow for different ways of data querying and interactive engagement, using a variety of JavaScript libraries and API's. Utilizing this mashup of visualization tools is merely the final stage in the development of the web-map. It is preceded first by extensive data analysis and manipulation of vast census and model output spatial data and second by creating a dedicated database in order to allow easy, intuitive and sometimes lateral querying of the database.

Figure 12: Time lapse visualization of various household socio-economic attributes on a dynamic web-map (see http://ccg.huji.ac.il/AgentBasedUrbanDisaster/index.html)

Figure 13: Time lapse visualization of the change in the number of passengers along roads on a dynamic web-map
(see http://ccg.huji.ac.il/AgentBasedUrbanDisaster/index.html)

7. Conclusions

This paper makes both a methodological and substantive contribution to the study of urban dynamics using recent advances in urban informatics and modeling. In terms of method we illustrate how an agent based model can be coupled with a data disaggregation process in order to produce synthetic big data with accurate socio-economic profiling. This fusion adds both temporal and spatial dynamics to the data. The simulation model uniquely treats the built environment as a quasi-agent in urban growth. Consequently, more attention is paid to the supply side dynamics of urban change than generally practiced and the result is a modeling system with dynamic pricing and an active supply side. We also illustrate how outputs can be suitably communicated to practitioners and the informed public. Dynamic web-based mapping is used to enhance civic engagement and public awareness as to the possible implications of a large scale exogenous shock.

On the substantive side the results of the simulation highlight some interesting urban processes at work. We speculate about three of them and their implications for the ability of cities to rejuvenate in the aftermath of an unanticipated event. The first relates to the permanent effects of temporary shocks. Our results have shown that temporary shocks to movement and traffic patterns can generate longer term lock-in effects. In our simulations these have a structural effect on reduction of CBD commercial activity. The issue arising here is the ability to identify when this fossilization takes place and when a temporary shock has passed the point of no return.

The second process relates to the large level of household turnover and 'churning' through the built fabric of the city in the aftermath of an earthquake. Obviously, a traumatic event serves to undermine population stability as housing stock is destroyed and citizens have to find alternative residence. However, high turnover levels of buildings point to a waste of resources, material, human and emotional. In other markets such as the labor market, 'churning' might be considered a positive feature pointing to economic and occupational mobility (Schettkat 1996). However, in the context of a disaster, this would seem to be a process that judicious public policy should attempt to minimize. The welfare costs of the effort needed to search for new accommodation and the dislocation associated with changing place of residence are likely fall hardest on weaker and more vulnerable populations (Felsenstein and Lichter 2014).

Finally, our findings shed new light on the familiar concept of 'urban vulnerability'. Our simulated results show that less vulnerable socio-economic groups 'weather the storm' by dispersing and then re-clustering over time. This points to their higher adaptive capacities. Stronger populations have the resources to accommodate the negative impacts of a disaster. Urban vulnerability is thus as much as an economic welfare issue as it an engineering or morphological concept. From a socioeconomic perspective, it is not the magnitude of the event that is important but the ability to cope with its results. This makes urban vulnerability a relative term: a shock of a given magnitude will affect diverse population groups differentially. Vulnerable populations or communities can be disproportionately affected by unanticipated disasters which are more likely to push them into crisis relative to the general population. Much of this can only be detected at the micro level such as the household. It is often smoke-screened in studies dealing with aggregate citywide impacts. The use of highly disaggregated and accurately profiled data would seem to be critical in understanding urban vulnerability.

Appendix 1: Data Disaggregation Method

This appendix describes the disaggregation procedure of spatially aggregated alpha numeric real-estate values and populations and their socio-economic attributes into discrete spatial units at the building level.

The number of floors in residential buildings (F_R), is calculated by dividing building height by average floor height of 5 m:

$$F_R = \frac{H_B}{5}$$

In the case of non-residential buildings, the number of floors (F_N) is estimated as the building height divided by average floor height of 5 m:

$$F_N = \frac{H_B}{7}$$

Floor space for each building (S_B) is then calculated by multiplying the number of floors in each building by its polygon area representing roof space:

$$S_B = S_R \times F$$

Where:
S_R= Building polygon footprint
F = Building number of floors

The GIS buildings layer and building type serve as the basis for the calculation of residential building value, non-residential building and equipment value. To create estimates of residential building value we use average house prices per m^2 2008-2013 (in real 2009 prices). In cases where no transactions exist in a specific SA over that period we use a regional estimate for residential property prices.

1.Value of residential buildings (P_{BR}) is calculated as follows:

$$P_{BR} = P_{SR} \times S_{BR}$$

where:
P_{SR} = Average SA price per m^2
S_{BR} = Residential building floor space.

2.Value of Non residential buildings is calculated as follows:

Non residential value per m^2 by region (P_{RN}):

$$P_{RN} = \frac{V_{RN}}{S_{RN}}$$

where:
S_{RN} = Total regional non residential floor space.
V_{RN}= Total regional non residential building stock

Non residential building value per m^2 for each region is multiplied by the floor space of each non-residential building to produce non-residential building values (P_{BN}):

$$P_{BN} = P_{RN} \times S_{BN}$$

where:
S_{BN} = non residential building floor space.

Regional non- residential stock estimates have been calculated for nine aggregate regions elsewhere (Beenstock et al. 2011).

3.Value of Equipment and Machinery (P_{RE}) is calculated as follows:

$$P_{RE} = \frac{V_{RE}}{S_{RN}}$$

where:
V_{RE}= Total regional non residential equipment stock

The equipment stock per m^2 for each region is multiplied by the floor space of each non-residential building to produce equipment stock totals by building (P_{BE}):

$$P_{BE} = P_{RE} \times S_{BN}$$

where:
S_{BN} = non residential building floor space.

The source for regional estimates of regional equipment and machinery stock is as above (Beenstock et al. 2011).

The buildings layer also allows for the spatial allocation of aggregated households, and population counts (see Table 1) into building level households and inhabitant totals. Given the existence of these spatial estimates, the distribution of aggregate average monthly earnings, participation in the work force, employment sector, disabilities and age (see Table 1) into a building level distribution is implemented.

4. Household density by SA (households per m^2) of residential floor space in a statistical area (H_{SR}) is calculated as follows:

$$H_{SR} = \frac{H_S}{S_{SR}}$$

where:
H_S= Total population per statistical area (IV in Table 1).
S_{SR} = Total statistical area residential floor space.

The number of households per building (H_B) is calculated as follows:

$$H_B = H_{SR} \times S_{BR}$$

5. Average number of inhabitants per m^2 of residential floor space in a statistical area (I_{SR}) is calculated as follows:

$$I_{SR} = \frac{I_S}{S_{SR}}$$

where:
S_{SR} = Total statistical area residential floor space.
I_S= Total population per statistical area.

Population counts per building (I_B) are then calculated as follows:

$$I_B = I_{SR} \times S_{BR}$$

6. Total earnings per building (M_B) is calculated as follows:

$$M_B = M_{SI} \times H_B$$

where:
M_{SI} = Average monthly earnings per household by SA.
H_B= Total number of households in a building.

7. Number of inhabitants in each building participating in the labor force 2008 (I_W) is calculated by multiplying the number of inhabitants in a building by the labor participation rate in the corresponding SA.

$$I_W = W_S \times I_B$$

where:
W_S = % of inhabitants participating in the labor force in an SA
I_B = Population count per building

8.Number of inhabitants per building by employment sector (I_O) is calculated by multiplying the percentage of inhabitants employed by sector (commercial, governmental, industrial or home-based) per statistical area by the number of inhabitants in each building.

$$I_O = O_S \times I_B$$

where:
O_S = % of inhabitants employed in an employment category.
I_B = Population counts per building

9 Number of disabled inhabitants in each building (I_D) is calculated by multiplying the number of inhabitants in a building by the percentage of disabled in the corresponding SA.

$$I_D = D_S \times I_B$$

where:
D_S = % of disabled inhabitants in an SA
I_B = Population count per building

10. Number of inhabitants in each age category (I_A) is calculated by multiplying the number of inhabitants in a building by the percentage of inhabitants in each age category in the corresponding SA.

$$I_A = A_S \times I_B$$

where:
A_S = % of inhabitants in each age group category in an SA
I_B = Population count per building.

Appendix 2: Behavioral Rules for the ABM

1. Residential Location Choice is derived as follows:

$$h_h = b_j \Rightarrow \left[\frac{I_h}{3} > HP_j\right] * \left[k_h > S(b_j)\right] = 1$$

where:

h_h is the new residential location for household *h*,

b_j is the building considered,

$[\ ]$ is a binary expression with value of 1 if true and 0 otherwise,

I_h is household *h*'s monthly income,

HP_j is monthly housing cost of an average apartment in building *j*,

k_h is a random number between [0,1] indicating tolerance to change in residential environment incurred by relocation,

$S(b_j)$ is a similarity score for building *j* in relation to current place of residence, calculated as follows:

$$S(b_j) = \frac{\Phi\left(\frac{\bar{I}_j - \bar{I}_h}{I_{\sigma_h}}\right) + \Phi\left(\frac{\bar{A}_j - \bar{A}_h}{A_{\sigma_h}}\right)}{2}$$

where:

Φ is the standard normal cumulative probability function,

$\bar{I}_j$, $\bar{A}_j$ are the average household income and average age of individuals in building *j*, respectively

$\bar{I}_h$, $\bar{A}_h$ are average household income and average age of individuals in residential buildings within 100 meter of current residential location of household *h*,

I_{σ_h}, A_{σ_h} are standard deviations of household income and of resident age in residential buildings within 100 meters from current home location of household *h*, respectively.

2. Choice of sequence of activities: occurs in two stages. First, the number of activities is fixed and then activities are allocated to locations:

$$\# Ac_i = \left\| a * \left(\frac{k_i}{0.5}\right) * (1 + car_h * 0.33) * (1 - dis_i * 0.33) * (1 + [age_i = 2] * 0.33) * (1 - [age_i \neq 2] * 0.33) \right\| + employed_i * here_i$$

where:

$\# Ac_i$ is the number of activities for resident *i*,

k_i is a randomly drawn number between [0,1] reflecting preferences regarding number of activities,

car_h is a binary variable equal to 1 if the household *h* owns a car and 0 otherwise,

dis_i is a binary variable equal to 1 if individual *i* is disabled and 0 otherwise,

age_i is the age group of individual *i*,

$employed_i$ is a binary variable equal to 1 if *i* is employed and 0 otherwise,
$here_i$ is a binary variable equal to 1 when *i*'s workplace is located within the study area and 0 otherwise,
$\|x\|$ indicates the nearest integer number to *x*,
a is the average number of activities based on employment status; equals 2.5 for employed residents and 3 for non-employed.

$$a_{t+1,i} = b_j \Rightarrow \lfloor b_j \neq a_{t,i} \rfloor * \lfloor k_i \geq Att(b_j) \rfloor = 1$$

where:

$a_{t,i}$ is the current location of individual *i*,
$a_{t+1,i}$ is the next location of activity of individual *i*,
k_i is a randomly drawn number between [0,1] reflecting activity location preferences,
$Att(b_j)$ is the attractiveness score for building *j*, calculated as follows:

$$Att(b_j) = \frac{1 - \Sigma E_j / \Sigma B_j + 1 - D_{ij} / \max D_i * (1 + 0.33 * (-car_h + dis_i + [age_i = 3])) + [LU_j = non\mathrm{Res}] * FS_j / \max FS}{2 + [LU_j = non\mathrm{Res}]}$$

where:

ΣE_j is the number of non occupied buildings within a 100 meter buffer of building *j*,
ΣB_j is the number of all buildings within a 100 meter buffer of building *j*,
D_{ij} is the distance of building *j* from the current location of individual *i*,
$\max D_i$ is the distance of the building within the study area furthest away from the current location of individual *i*,
LU_j is the land-use of building *j*,
nonRes is non-residential use,
FS_j is the floor-space volume of building *j*,
maxFS is the floor-space volume of the largest non-residential building within the study area.

3. Choice of workplace location is calculated similarly to the choice of activity location:

$$WP_i = b_j \Rightarrow \lfloor LU_j = ELU_i \rfloor * \left\lfloor k_i > \frac{D_{ij} / \max D_i + 1 - FS_j / \max FS}{2} \right\rfloor = 1$$

where:

WP_i is the workplace location of individual *i*,
ELU_i is the employment-sector-related land-use for individual *i*,
k_i is a randomly drawn number between [0,1] representing workplace location preferences,

D_{ij} is the distance between building *j* and individual *i*'s place of residence,

$\max D_i$ is the distance of the building within the study area furthest away from individual *i*''s place of residence.

4.Building values and the monthly cost of living in a dwelling unit are derived in a 3-stage process. First, daily change in average house price per SA is calculated. Then, values of individual buildings are derived and finally the price of the single, average dwelling unit is calculated. For non-residential buildings, the calculation of individual building values is similar.

$$AHP_{z,t+1} = AHP_{z,t} * \left(1 + \log\left(\frac{{pop_{z,t+1}}/{pop_{z,t}} + {res_{z,t}}/{res_{z,t+1}} + {n\mathrm{Re}s_{z,t+1}}/{n\mathrm{Re}s_{z,t}}}{3}\right)\right)$$

$$ANRV_{z,t+1} = ANRV_{z,t} * \left(1 + \log\left(\frac{n\mathrm{Re}s_{z,t}}{n\mathrm{Re}s_{z,t+1}}\right)\right)$$

where:

$AHP_{z,t}$ is average housing price per meter in SA *z* at time *t*,

$pop_{z,t}$ is population in SA *z* at time *t*,

$res_{z,t}$ is the number of residential buildings in SA *z* at time *t*,

$n\mathrm{Re}s_{z,t}$ is the number of non-residential buildings in SA *z* at time *t*,

$ANRV_{z,t}$ is the average non-residential value per meter in SA *z* at time *t*,

$$HP_{j,t} = AHP_{z,t} * FS_j * {SL_{j,t}}/{SL_{z,t}}$$

$$V_{j,t} = ANRV_{z,t} * FS_j$$

where:

$HP_{j,t}$ is the house price of a dwelling unit in building *j* at time *t*,

$SL_{s,t}$ is the service level within area *s* at time *t* – the ratio of non-residential buildings to residential buildings in this perimeter,

$V_{j,t}$ is the non-residential value of building *j*.

$$P_{du,t} = \frac{\bar{I}_t * \left(1 + \frac{{HP_{j,t}}/{\Sigma Ap_j} - {\sum_{l=1}^{L_t} HP_{l,t}}/{\sum_{l=1}^{L_t} \Sigma Ap_l}}{P_{\sigma_t}}\right)}{c}$$

where:

$P_{du,t}$ is the monthly cost of living in dwelling unit *du* at time *t*,

$\bar{I}_t$ is the average household income in the study area at time *t*,

ΣAp is the number of dwelling units within a building. If the building is initially of residential use, this is equal to its initial population size, otherwise it is the floor-space volume of the building divided by 90 (assumed to be average dwelling unit size in meters),

L_t is the number of residential buildings in the study area at time *t*,

P_{σ_t} is the standard deviation of dwelling unit prices within the study area at time *t*,

c is a constant.

5. *Land-use changes*, from residential to commercial and from commercial to unoccupied are based on the congruence between the building floor-space volume and the average intensity of traffic on roads within a 100 m radius over the preceding 30 days. Both these values are compared with the (assumed) exponential distribution of all values in the study area. This is done by computing the logistic probability of the relative difference in their locations in the distribution:

$$P_{j,t}\left(\Delta x_{j,t}\right) = \frac{e^{-\Delta x_{j,t}}}{1+e^{-\Delta x_{j,t}}}$$

$$\Delta x_{j,t} = \frac{z_{TR_{j,t}} - z_{FS_{t,t}}}{\left|z_{FS}\right|}$$

$$z_{y_{t,j}} = \frac{e^{-y_{j,t}/\bar{y}_t} - e^{-y_{med_t}/\bar{y}_t}}{\bar{y}_t}$$

where:

$P_{j,t}$ is the probability of land-use change for building *j* at time *t*,

$\Delta x_{j,t}$ is the relative difference in position of traffic load and floor-space for building *j* at time *t*,

$z_{y\ j,t}$ is the position of value *y* in the exponential distribution, relative to the median for building *j* at time *t*,

$\dfrac{e^{-y_{j,t}/\bar{y}_t}}{\bar{y}_t}$ is the exponential probability density value for *y* ($\dfrac{1}{\bar{y}_t} = \hat{\lambda}_t$) for building *j* at time *t*,

y_{med_t} is the median of *y* at time *t*.

If *P>0.99* for residential use, it changes to commercial. If the value is in the range [*P(1)-0.01,P(1)*] for commercial uses, the building becomes unoccupied. This functional form and criteria values reduce the sensitivity of large commercial uses and small residential uses to traffic volume. Consequently, the process of traffic-related land-use change is not biased by a tendency to inflate initial land uses.

6. Earthquake impact is calculated as follows:

$$\mathrm{Im}_j = \frac{c * 10^{mag}}{D_j * \left|\log(D_j)\right| * F_j}$$

where:

Im_j is the impact building *j* suffers, c is a constant, *mag* is the earthquake magnitude (similar to Richter scale), D_j is distance of building *j* from the earthquake epicenter, F_j is number of floors in building *j*..

References

Batty M, Hudson-Smith A, Milton R, and Crooks A (2010) Map Mashups, Web 2.0 and the GIS Revolution, *Annals of GIS,* 16 (1), 1–13.

Beenstock M, Felsenstein D and Ben Zeev NB (2011) Capital deepening and regional inequality: an empirical analysis, *Annals of Regional Science*, 47, 599-617

Chang, SE (2003). Transportation planning for disasters: An accessibility approach, *Environment and Planning A*, 35(6), 1051–1072

Chen X, Meaker JW and Zhan FB (2006). Agent-based modeling and analysis of hurricane evacuation procedures for the Florida Keys, *Natural Hazards*, 38, 321–338.

Chen, X and Zhan, FB (2008). Agent-based modeling and simulation of urban evacuation: Relative effectiveness of simultaneous and staged evacuation strategies, *Journal of the Operational Research Society*, 59, 25–33.

Crooks AT and Wise S (2013) GIOS and Agent Based Models for Humanitarian Assistance, *Computers Environment and Urban Systems*, 41, 100-111.

Dawson RJ., Peppe R and Wang M (2011) An agent-based model for risk-based flood incident Management, *Natural Hazards* 59,167–189.

Eicher, CL and Brewer, CA (2001). Dasymetric mapping and areal interpolation: implementation and evaluation, *Cartography and Geographic Information Science,* 28 (2), 125-138

Felsenstein D and Lichter M (2014) Social and Economic Vulnerability of Coastal Communities to Sea Level Rise and Extreme Flooding, *Natural Hazards*, 71, 463-491

Fiedrich, F., & Burghardt, P. (2007). Agent-based systems for disaster management, *Communications of the ACM*, 50(3), 41–42.

Grinberger AY and Felsenstein D (2014) Bouncing Back or Bouncing Forward? Simulating Urban Resilience, *Urban Design and Planning*, 167(3), 115-124.

Grinberger AY and Felsenstein D (2015) A Tale of Two Earthquakes: Dynamic Agent-Based Simulation of Urban Resilience, in Clarke G and Stern E (eds) *Applied GIS and Spatial Modeling*. Taylor and Francis (forthcoming).

Harper G and Mayhew L (2012a) Using Administrative Data to Count Local Populations, *Journal of Applied Spatial Analysis and Policy,* 5 (2), 97–122

Harper G and Mayhew L (2012b) R*e-thinking households – Using administrative data to count and classify households with some applications*. Actuarial Research Paper, No. 198. Cass Business School, London

Keon D, Steinberg B, Yeh H, Pancake CM and Wright D (2014) Web-based spatiotemporal simulation modeling and visualization of tsunami inundation and potential human response, *International Journal of Geographical Information Science*, 28(5), 987-1009, Kwan, MP and Lee J (2005). Emergency response after 9/11: The potential of realtime 3D GIS for quick emergency response in micro-spatial environments, *Computers, Environment and Urban Systems*, 29, 93–113.

Lichter M and Felsenstein D (2012) Assessing the Costs of Sea Level Rise and Extreme Flooding at the Local Level; A GIS-Based Approach, *Ocean and Coastal Management,* 59, 47-62

Linard C, Gilbert M, and Tatem, AJ (2011).Assessing the use of global land cover data for guiding large area population distribution modeling *GeoJournal*, 76 (5), 525-538.

Macal, CM, and North, MJ (2005). Tutorial on agent-based modeling and simulation, in *Proceedings of the 37th conference on Winter simulation*. WSC '05. Winter Simulation Conference, 2-15.

Mennis, J (2003), Generating surface model of population using dasymetric mapping, *The Professional Geographer*, 55(1), 31-42.

Oliveira, MGS, Vovsha, P, Wolf, J, Birotker, Y, Givon, D, and Paasche, J (2011). Global Positioning System-Assisted Prompted Recall Household Travel Survey to Support Development of Advanced Travel Model in Jerusalem, Israel, *Transportation Research Record: Journal of the Transportation Research Board,* 2246(1), 16-23.

Rashed T, Weeks J, Couclelis H and Herold M (2007) An integrative GIS and remote sensing model for place-based urban vulnerability analysis, in Mesev V (ed) *Integration of GIS and Remote Sensing* (pp 199-231). John Wiley & Sons, Ltd.

Reibel M and Bufalino ME (2005) Street-weighted interpolation techniques for demographic count estimation in incompatible zone systems, *Environment and Planning A*, 37,127-139.

Salamon A, Katz O and Crouvi O (2010). Zones of required investigation for earthquake-related hazards in Jerusalem, *Natural Hazards*, 53(2), 375-406.

Schettkat R (1996) *Flows in Labor Markets: Concepts and International Comparative Results,* in Schettkat R (ed) *The Flow Analysis of Labor Markets* (pp. pp 14-36). Routledge London.

Simoes J A (2012) An agent Based/ Network Approach to Spatial Epidemics, in Heppenstall AJ, Crooks AT, See LM and Batty M (eds) *Agent-Based Models of Geographical Systems* (pp 591-610). Springer, Netherlands.

Torrens PM (2014) High-resolution space-time processes for agents at the Built-human interface of urban earthquakes, *International Journal of Geographical Information Science*, 28(5), 964-986,

Zou Y, Torrens PM, Ghanem RG and Kevrekidis IG (2012) Accelerating agent-based computation of complex urban systems, *International Journal of Geographical Information Science*, 26(10), 1917-1937.